Science Bulletin 64 (2019) 718–722

Contents lists available at ScienceDirect

Science Bulletin

journal homepage: www.elsevier.com/locate/scib

Short Communication

A three-dimensional hollow graphene fiber microelectrode with shrink-effect-enabled enzyme immobilization for sensor applications

Liwei Chen [a], Xiaoteng Ding [b], Jinfeng Zeng [a], Le Jiao [a], Chongbei Wu [a], Yuze Wang [a], Qing Han [a,*], Liangti Qu [a]

[a] Key Laboratory of Photoelectronic/Electrophotonic Conversion Materials, Key Laboratory of Cluster Science, Ministry of Education of China, School of Chemistry and Chemical Engineering, Beijing Institute of Technology, Beijing 100081, China
[b] College of Life Sciences, Qingdao University, Qingdao 266071, China

ARTICLE INFO

Article history:
Received 15 February 2019
Received in revised form 3 April 2019
Accepted 18 April 2019
Available online 25 April 2019

Microelectrodes are a type of electrode with microscopic dimension, and due to their rapid diffusing rates, high electrical current densities and signal-to-noise ratios, they can help improve the detection sensitivity for various analytes [1]. Investigations on the fabrication and the application of microelectrodes are highly relevant. Fiber-type microelectrodes with one-dimensional (1D) microstructures that possess 1D diffusion, particularly carbon fiber microelectrodes, have been widely fabricated and used in many different types of sensors due to their low cost, small volume, portability, and good biocompatibility [1,2]. However, poor electrocatalytic activity and low response currents preclude the applications of carbon fiber microelectrodes in sensors.

Due to its high electron mobility, large specific surface area and excellent mechanical performance, graphene has aroused much interest for the synthesis of highly effective electrochemical sensors since it was discovered [3]. We recently reported a nitrogen-doped graphene fiber, which exhibited enhanced sensor performance but suffered from low interfacial area and poor mechanical performance due to its cylindrical structure [2]. Porous three-dimensional (3D) graphene architecture has a greater interior area and more active sites, resulting in remarkable electrocatalytic activity, thus enhancing the performance of devices such as electrochemical sensors, photovoltaic cells and supercapacitors [3,4]. Additionally, a hollow interior has been proposed to provide a larger specific surface area, thereby increasing electrode-electrolyte interfacial contact and promoting electron transport, as well as improving the mechanical properties [5]. These advantages make porous 3D graphene and the hollow graphene fiber excellent electrode materials for electrochemical analysis.

Electrochemical enzyme sensors integrate the high specificity of enzyme-catalyzed reactions with the high sensitivity of electrochemical signal detection and have been rapidly developed and widely applied over the last three decades [6]. Enzyme immobilization is an effective way to achieve reusable enzymes and improve stability. In general, enzymes are immobilized by covalent bonding through functional groups or noncovalent interactions (i.e., van der Waals forces and hydrogen bonding), causing many problems, such as deterioration of the activity stability and shorter service cycle [6,7]. The focus of enzyme immobilization is to develop new carrier materials and to design simple and convenient immobilized method that utilize extremely mild conditions.

It was recently reported that the hydration and/or dehydration of graphene-based materials could trigger the deformation of graphene sheets [8], which is potentially profitable for enzyme immobilization. Based on these concepts, we present an electrochemical enzyme sensor based on a 3D porous graphene coated hollow graphene fiber (PHGF) via a simple and effective shrink-effect-enabled enzyme immobilization method. As a micro-enzyme electrode for glucose, the PHGF microelectrode (PHGFM) shows good immobilization of glucose oxidase (GOD), which retains its catalytic activity, thus leading to high sensitivity, selectivity and long-term stability for the detection of glucose. As shown in Fig. 1, the removable Cu wire (Fig. 1a) acted as a core for the succeeding formation of the tubular structure and was immersed into a graphene oxide (GO) suspension. After drying, chemically reduced graphene oxide (RGO) aggregated along the Cu wire (RGO/Cu, Fig. 1b) due to the spontaneous redox reaction between GO and Cu [8]. The etching of Cu wire in a mixture of $FeCl_3$ and HCl aqueous solution resulted in the formation of hollow graphene fiber (Fig. 1c). The subsequent electrochemical reduction of GO on the hollow graphene fiber in aqueous dispersion directly generated 3D porous graphene coated hollow graphene fiber, which was denoted as PHGF (Fig. 1d). The

* Corresponding author.
E-mail address: qhan@bit.edu.cn (Q. Han).

https://doi.org/10.1016/j.scib.2019.04.031
2095-9273/

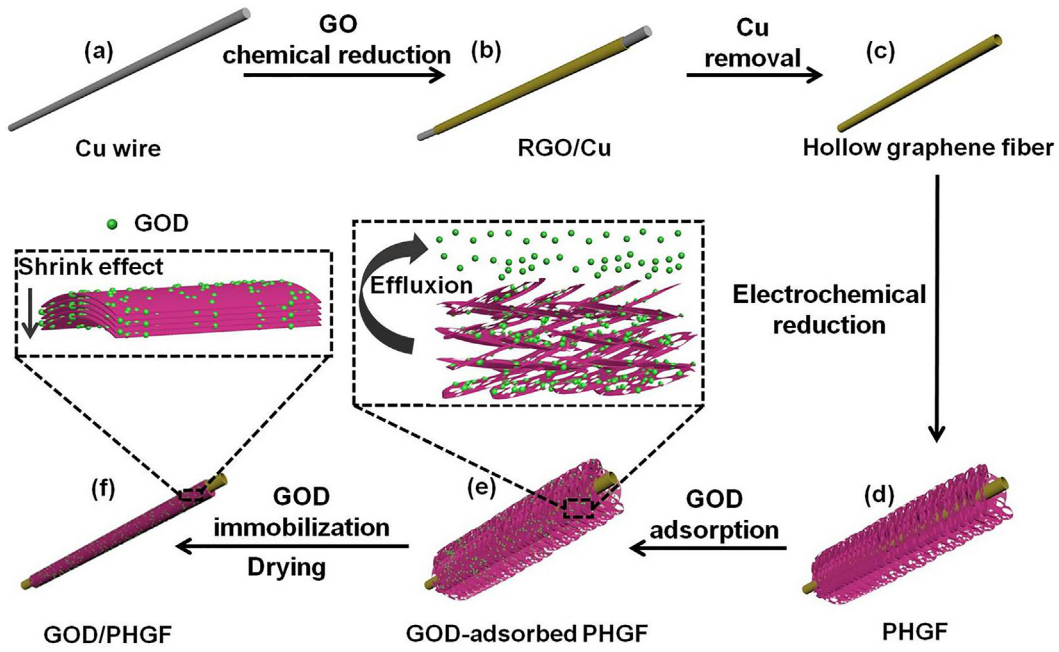

Fig. 1. Experimental procedure for the fabrication of GOD/PHGF. (a) Cu wire; (b) RGO/Cu; (c) Hollow graphene fiber; (d) PHGF; (e) GOD-adsorbed PHGF; (f) GOD/PHGF.

porous structure of 3D graphene provided countless binding sites for GOD adsorption when the PHGF was impregnated in GOD solution. After the absorption of GOD, the GOD-adsorbed PHGF was formed (Fig. 1e). Then, dehydration-responsive shrinking of graphene sheets in the 3D graphene occured in the following drying process due to the stretching and rotating of carbon-carbon bonds [8]. In this way, GOD was successfully immobilized on the PHGF (named as GOD/PHGF, Fig. 1f).

Scanning electron microscopy (SEM) images show that the pristine hollow graphene fiber has a hollow fiber structure with a diameter of 50 μm (Fig. 2a–c), illustrating the successful replication of the copper wire shape. It is clear from Fig. 2b that the surface of hollow graphene fiber is rough and full of wrinkles sheet-like morphologies. By contrast, PHGF is a hollow fiber with a diameter of 240 μm that is wrapped with 3D interconnected graphene networks (Fig. 2d–f). After automatic adsorption and immobilization of GOD, the morphology of PHGF was dramatically altered, resulting in the hollow fiber morphology of GOD/PHGF (Fig. 2g–i), similar to the pristine hollow graphene fiber. Notably, the GOD/PHGF wall consists of densely packed graphene sheets (the rectangular area in Fig. 2i), which is significantly thicker than that of the pristine hollow graphene fiber (the rectangular area in Fig. 2c), indicating shrinking of graphene sheets in the 3D graphene occurred during drying, thus immobilizing GOD in the pores of PHGF.

X-ray diffraction (XRD) patterns (Fig. S1 online) show that, in contrast to the calculated interlayer spacing of approximately 0.77 nm for GO, PHGF has an interlayer spacing of 0.34 nm, suggesting the reduction of GO sheets in PHGF. X-ray photoelectron spectroscopy (XPS) spectra in Fig. 2j show that the C/O atomic ratio increases from 2.51 for GO to 11.14 for PHGF (Table S1 online), demonstrating a significant reduction of oxygenic groups in PHGF. In addition, the peaks associated with the oxidized carbon species (C–O at 286.6 eV and C=O at 288.5 eV) [9] in PHGF were much less intense (Fig. 2k) than those of GO, further indicating that many of the oxygen-containing groups were removed.

The electrochemical properties of $Fe[(CN)_6]^{3-}$ at hollow graphene fiber microelectrode (HGFM) and PHGF microelectrode (PHGFM) were investigated. As shown in Fig. 2l, both scans exhibited sigmoid-shaped peaks, suggesting spherical diffusion on the microelectrodes. The diffusion limit current of PHGFM was almost 20 times that of HGFM, which can be attributed to a larger surface area due to the 3D porous structure of PHGFM, thereby providing more adsorption sites for GOD.

The direct electrochemistry of GOD at GOD-immobilized PHGFM (GOD/PHGFM) was tested in 0.1 mol L^{-1} phosphate buffered saline (PBS). Meanwhile, HGFM, GOD absorbed HGFM (GOD/HGFM), and PHGFM were studied for comparison (Fig. 3a). Clearly, there is no obvious peak for GOD/HGFM, which can be attributed to the lack of 3D porous graphene on the surface of HGFM, so enzyme cannot be effectively adsorbed and immobilized. In contrast, GOD/PHGFM exhibits an apparent redox couple with a formal potential ($E^{0'}$) of –0.47 V, which is very close to the standard potential for $FADH_2$/FAD (–0.46 V, the redox active sites of GOD) [10]. This demonstrates that there was no denaturation of GOD on the surface of GOD/PHGFM and that direct electron transfer occurred effectively and steadily (Fig. 3a). Meanwhile, $E^{0'}$ depends linearly on the electrolyte pH value with a slope of 57 mV pH^{-1}, and both the anodic and cathodic peak currents of GOD/PHGFM are linear with the square root of the scan rate, demonstrating a $2e/2H^+$ transfer and surface-controlled electrochemical process between the electrode and the enzyme (Figs. S4a, S4b and Eq. (S1) online). These results demonstrate the successful immobilization of GOD through the dehydration-induced shrinking of 3D porous graphene, as well as the retention of GOD activity.

To testify the electrocatalytic activity of GOD, differential pulse voltammetry curves (DPVs) were firstly measured in N_2-saturated PBS and then in air-saturated PBS with or without 0.1 mmol L^{-1} glucose. As shown in Fig. 3b, the cathodic peak current (I_c) of GOD/PHGFM in air-saturated PBS is larger than that in N_2-saturated solution, which is due to the catalysis of O_2 on GOD ($FADH_2$) (Eq. (S2) online). After adding glucose in air-saturated PBS, I_c decreases owing to the reduction of the amount of GOD (FAD) in the solution. This is caused by the catalytic oxidation-reduction for glucose (Eq. (S3) online) and further supports the need for 3D graphene shrinking during enzyme immobilization. Hence, when glucose concentration increases from 0 to 8 mmol L^{-1}, the I_c of GOD/PHGFM gradually decreases (Fig. 3c). These results

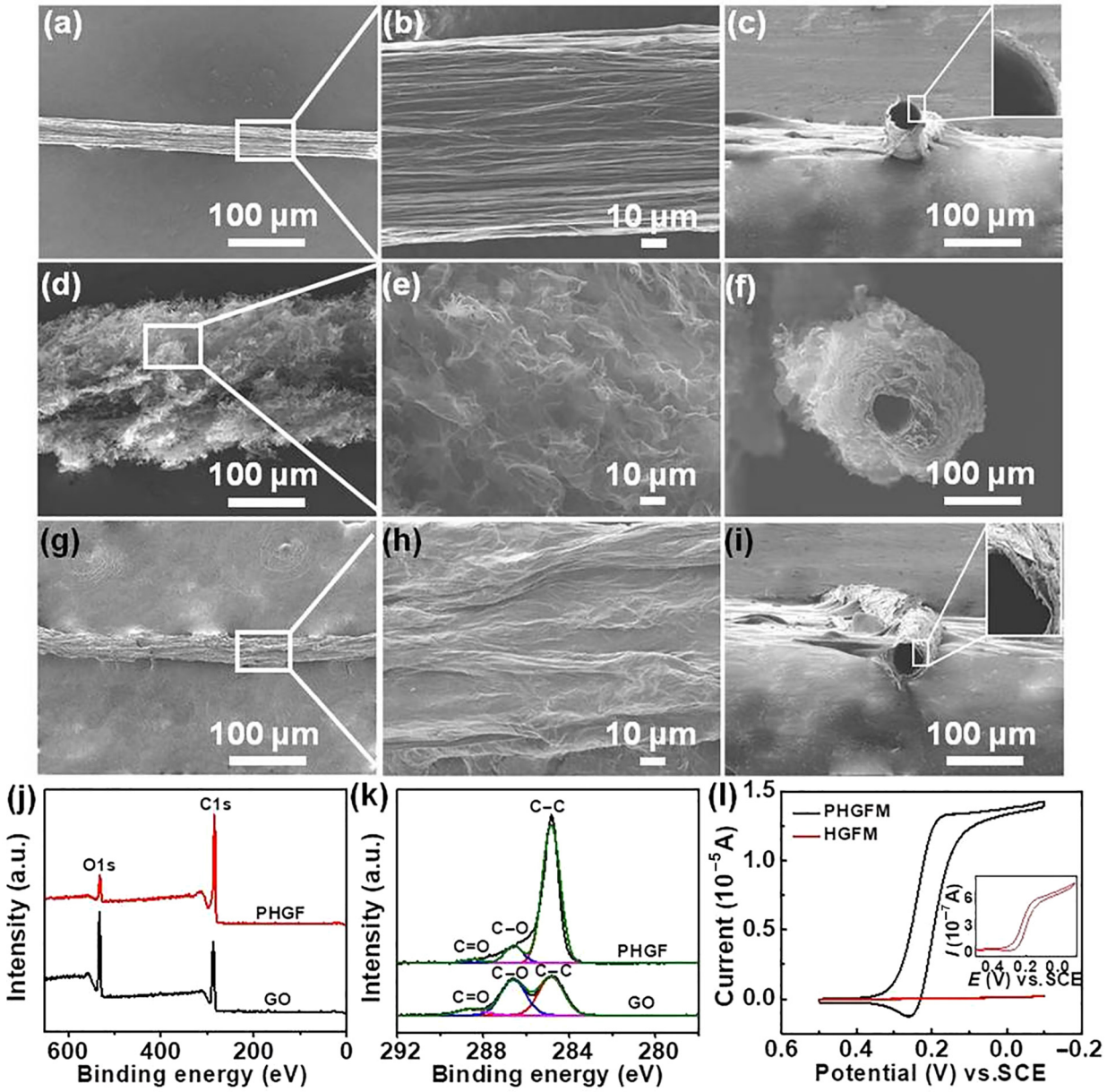

Fig. 2. SEM images of a hollow graphene fiber (a), PHGF (d), GOD/PHGF (g); (b, e, h) The corresponding magnified views of the rectangular areas in (a, d, g); SEM images of the cross sections of a hollow graphene fiber (c), PHGF (f) and GOD/PHGF (i). (j) XPS survey spectra of GO and PHGF. (k) High-resolution XPS spectra of carbon species of GO and PHGF. (l) Cyclic voltammetry (CV) curves of HGFM and PHGFM in the aqueous solution of 0.5 mol L^{-1} KCl containing 5.0 mmol L^{-1} $K_3Fe[(CN)_6]$, a saturated calomel reference electrode (SCE) and a platinum plate counter electrode; Insert: the enlarged CV curve of HGFM, scan rate: 5 mV s^{-1}.

suggest that 3D porous structure of GOD/PHGFM provided a favorable bioenvironment that maintained the catalytic activity of GOD towards glucose detection. As a result, GOD/PHGFM shows two good linear responses for glucose detection: an ultrahigh sensitivity of 148.02 μA mmol L^{-1} cm^{-2} in the range of 0.01–1 mmol L^{-1}, and a good sensitivity of 22.25 μA mmol L^{-1} cm^{-2} in the range of 1–8 mmol L^{-1} (Fig. 3d). These two linear relationships could presumably be elucidated as a "multi-layer adsorption mechanism" in GOD caused by the 3D porous structure on GOD/PHGFM [10]. At low concentrations, glucose is catalyzed by the internally immobilized GOD with a short path and low energy barrier for electron transfer. However, at high concentrations, the externally immobilized GOD with a longer path and higher energy barrierfor electron transfer also participates in the reaction, which leads to a relatively low sensitivity. The detection limit obtained for GOD/PHGFM was estimated to be 3.3 μmol L^{-1} (S/N = 3). In contrast to other reported GOD electrodes (Table S2 online), GOD/PHGFM shows a wider linear range and a greater response.

GOD/PHGFM shows no obvious change in the peak current or peak potential in the presence of distractions, such as dopamine (DA), hydrogen peroxide (H_2O_2) and ascorbic acid (AA) (Fig. 3e), indicating a high selectivity for glucose. The peak current barely changed after 100 cycles (Fig. S5a online), indicating that the enzyme is stably immobilized on the electrode. In addition, after 100-cycles stability testing, GOD/PHGFM shows similar diameter and appearance as its original state (Fig. S5b and c online), revealing that the graphene structure remains its state of shrinkage when placed back into an aqueous solution. GOD/PHGFM remains 90% of its original response after storing for two weeks at 4 °C (Figs. 3f and S5d online), suggesting that the enzyme is securely immobilized, thus exhibiting good activity and stability. The reproducibility was investigated by testing six GOD/PHGFM samples simultane-

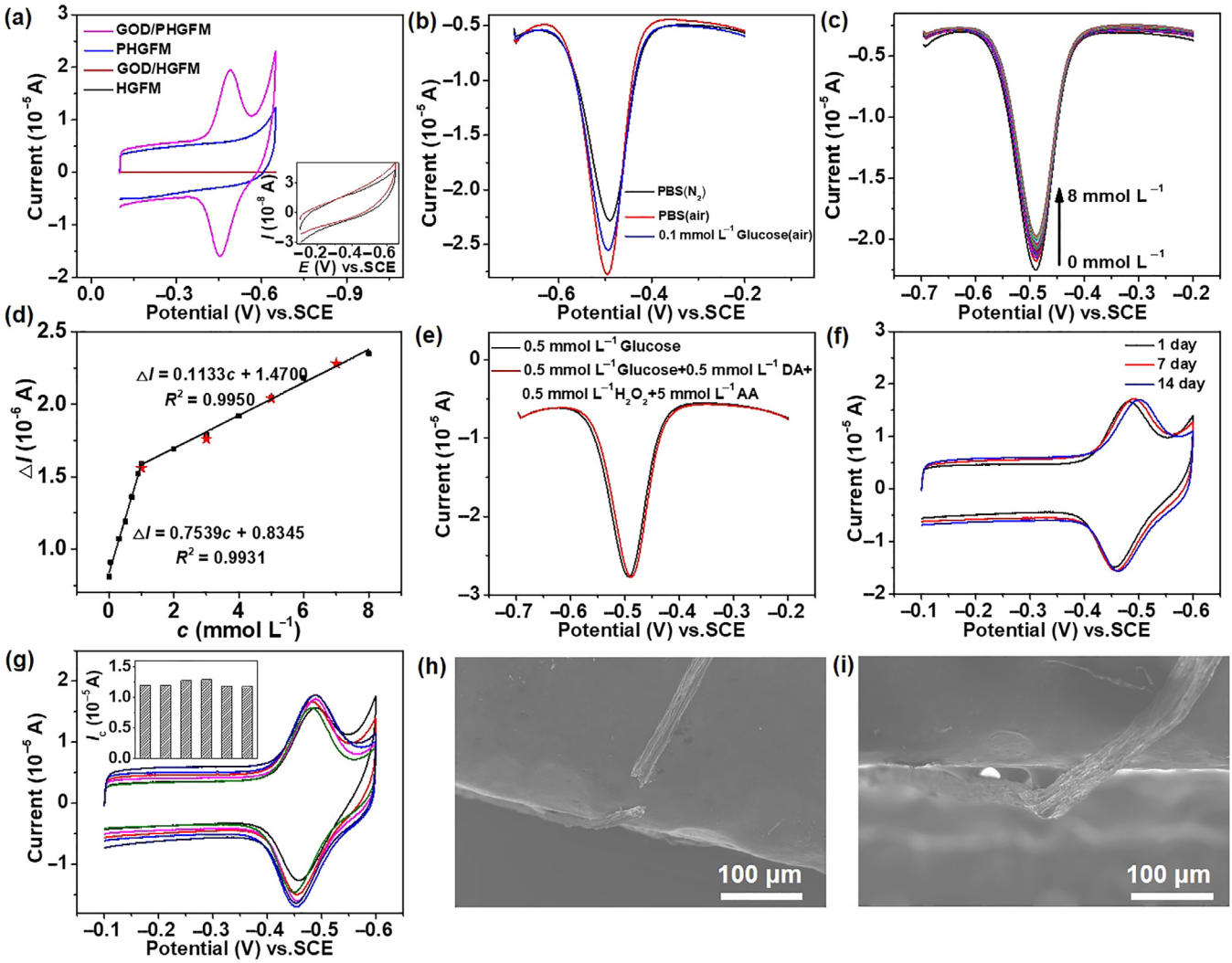

Fig. 3. The electrochemistry, detection performance and mechanical properties of GOD/PHGFM. (a) CV curves of HGFM, GOD/HGFM, PHGFM and GOD/PHGFM in 0.1 mol L^{-1} PBS (pH 7.0), insert: enlarged CVs of HGFM and GOD/HGFM, scan rate: 50 mV s^{-1}. (b) DPVs of GOD/PHGFM in N_2-saturated PBS and air-saturated PBS (pH 7.0) with or without 0.1 mmol L^{-1} glucose. (c) DPVs of GOD/PHGFM in air-saturated 0.1 mol L^{-1} PBS containing glucose with different concentrations: 0, 0.01, 0.05, 0.1, 0.2, 0.3, 0.4, 0.5, 0.6, 0.7, 0.8, 0.9, 1.0, 2.0, 3.0, 4.0, 5.0, 6.0, 7.0 and 8.0 mmol L^{-1}. (d) The calibration curves of the reductive value of cathodic peak current vs. glucose concentrations in 0.01–1 mmol L^{-1} and 1–8 mmol L^{-1}. The red stars represent the reductive values of cathodic peak current measured at the concentrations of 1, 3, 5, and 7 mmol L^{-1} in human serum samples. (e) DPVs of GOD/PHGFM in 0.5 mmol L^{-1} glucose solution and 0.5 mmol L^{-1} glucose solution containing 0.5 mmol L^{-1} DA, 0.5 mmol L^{-1} H_2O_2 and 5 mmol L^{-1} AA. (f) CV curves of GOD/PHGFM after differential storage period in N_2-saturated PBS (0.1 mmol L^{-1}, pH 7.0). (g) CV curves of six parallel GOD/PHGFM in N_2-saturated PBS (0.1 mmol L^{-1}, pH 7.0). The inset shows the histogram of the cathodic peak current (I_c) of the six microelectrodes; SEM images of graphene fiber (h) and GOD/PHGF (i) bent at an angle of 90°. In all the electrochemical tests mentioned above, a saturated calomel electrode (SCE) and a platinum plate electrode were used as the reference and counter electrodes, respectively.

ously, and a 3.9% relative standard deviation (RSD) were calculated (Fig. 3g), indicating that the high activity is reproducible. Notably, the hollow interior structure of the GOD/PHGFM endows it with high mechanical strength, even when bent three times to an angle of 90° (Figs. 3i and S6d–f online). However, the cylindrical graphene fiber broken when bent to the same angle (Fig. 3h), indicating that the unique inner structure of the hollow fiber can provide enough space to compensate for buckling of the fiber. In addition, the Nyquist plots in Fig. S7 (online) show that the conductivity of the fiber hardly changes before and after bending at 90°. Therefore, the fiber with a hollow structure is able to tolerate large deformations without damage. The GOD/PHGFM was further used for glucose detection at different concentrations (1, 3, 5 and 7 mmol L^{-1}) in human serum (Fig. S8 online). The recovery rate (Table S3 online) was calculated according to calibration curves (Fig. 3d) and was in the range of 90.00%–108.82%, proving that GOD/PHGFM is effective for the glucose detection in human serum samples. By altering the adsorption and drying time of GOD in the fiber, an optimal microelectrode with the highest electrocatalyic activity was obtained (Figs. S1–S3 online).

In summary, an electrochemical biosensor for glucose has been developed by shrink-effect-enabled enzyme immobilization of GOD enzyme in the pores of 3D graphene on the surface of a hollow graphene fiber microelectrode. The 3D porous structure and hollow fiber interior of the microelectrode give rise to increased adsorption sites for enzymes, enhanced electric transmission and well-immobilized, robust enzymes with high reactivity. This results in a good electroanalytical performance for glucose detection. This work provides a facile enzyme immobilization method for designing novel microelectrodes for in vitro or in vivo analysis.

Conflict of interest

The authors declare that they have no conflict of interest.

Acknowledgments

This work was supported by the National Natural Science Foundation of China (21575014), Beijing Natural Science Foundation (2184122), the Fundamental Research Funds for the Central Universities (2018CX01017), Beijing Institute of Technology Research Fund Program for Young Scholars, the Project of State Key Laboratory of Explosion Science and Technology (Beijing Institute of Technology, YBKT18-03), and Analysis & Testing Center, Beijing Institute of Technology.

Author contributions

Q. H. supervised the entire project. Q. H. and L. C. conceived the idea and co-wrote the paper. L. C. performed the whole material preparation and characterization and carried out data analyses. X. D., J. Z., L. J., C. W. and Y. W. gave advices on the experiments and reviewed the paper. All the authors discussed the results and commented on the paper.

Appendix A. Supplementary data

Supplementary data to this article can be found online at https://doi.org/10.1016/j.scib.2019.04.031.

References

[1] Chandra S, Siraj S, Wong D. Recent advances in biosensing for neurotransmitters and disease biomarkers using microelectrodes. ChemElectroChem 2017;4:1–13.
[2] Ding X, Bai J, Xu T, et al. A novel nitrogen-doped graphene fiber microelectrode with ultrahigh sensitivity for the detection of dopamine. Electrochem Commun 2016;72:122–5.
[3] Hondred J, Medintz I, Claussen J. Enhanced electrochemical biosensor and supercapacitor with 3D porous architectured graphene via salt impregnated inkjet maskless lithography. Nanoscale Horiz 2019;4:735–46.
[4] Huang G, Han J, Zhang F, et al. Lithiophilic 3D nanoporous nitrogen-doped graphene for dendrite-free and ultrahigh-rate lithium-metal anodes. Adv Mater 2019;31:1805334.
[5] Qu G, Cheng J, Li X, et al. A fiber supercapacitor with high energy density based on hollow graphene/conducting polymer fiber electrode. Adv Mater 2016;28:3646–13252.
[6] Adeel M, Bilal M, Rasheed T, et al. Graphene and graphene oxide: functionalization and nano-bio-catalytic system for enzyme immobilization and biotechnological perspective. Int J Biol Macromol 2018;120:1430–40.
[7] Hondred J, Breger J, Alves N, et al. Printed graphene electrochemical biosensors fabricated by inkjet maskless lithography for rapid and sensitive detection of organophosphates. ACS Appl Mater Interfaces 2018;10:11125–34.
[8] Xu T, Han Q, Cheng Z, et al. Interactions between graphene-based materials and water molecules toward actuator and electricity-generator applications. Small Method 2018;2:1800108.
[9] Zhao F, Cheng H, Zhang Z, et al. Direct power generation from a graphene oxide film under moisture. Adv Mater 2015;27:4351–7.
[10] Richards EG. Biology's conscience. Nature 1986;319:804.

Liwei Chen obtained her Bachelor's degree from the Taiyuan University of Technology in 2016. She is now a graduate student in the School of Chemistry and Chemical Engineering at Beijing Institute of Technology under the supervision of Assistant Prof. Qing Han. Her current research focuses on fabrication and application of graphene-based microelectrode sensors.

Qing Han is an assistant professor of Chemistry at Beijing Institute of Technology (Beijing, China). She received a Ph.D. degree in Chemistry from Beijing Institute of Technology. Her research focuses on (i) design and synthesis of nanocatalysts for photocatalysis and electrocatalysis as well as (ii) device fabrication of carbon-based nanomaterials for energy conversion/storage applications.